Search for an Electron Mass Shift in ^{133}Cs in an Intense Electromagnetic Field*

J. RICHARD MOWAT,† CHARLES E. JOHNSON, AND HOWARD A. SHUGART
Department of Physics and Lawrence Radiation Laboratory, University of California, Berkeley, California 94720

AND

VERNON J. EHLERS
Department of Physics, Calvin College, Grand Rapids, Michigan 49506

(Received 10 November 1969; revised manuscript received 3 August 1970)

The possibility that the mass of a bound electron changes when placed in an intense electromagnetic field is studied here both theoretically and experimentally. The atomic-beam magnetic-resonance technique was used to examine hyperfine-structure frequency shifts in ^{133}Cs that occur when the atom is subjected to an intense, nonresonant radio-frequency magnetic field perpendicular to the static "C" field. A 2921-MHz TM_{010} cavity produced the perturbing field and was situated between Ramsey separated oscillatory loops, which induced the resonant transitions of interest. Shifts were observed for six $\Delta m_F = \pm 1$ transitions at field-independent points. No evidence was found for an electron mass shift. Good agreement is found between all observed shifts and those expected from a multilevel Bloch-Siegert effect.

I. INTRODUCTION

IT has been suggested[1] that, when an electron interacts with a classical, plane-polarized electromagnetic field, a finite mass renormalization occurs such that the electron's observable mass increases, becoming

$$m_* = \left[m_0^2 + \frac{1}{2}\left(\frac{ea}{c^2}\right)^2 \right]^{1/2} \simeq m_0 + \frac{1}{4}\frac{e^2a^2}{m_0c^4}, \qquad (1)$$

where m_0 is the electron rest mass in the absence of the field, e is the electron charge, c is the speed of light in vacuum, and a is the (real) scalar amplitude of the vector potential describing the field. The relative mass shift is defined by

$$\frac{m_* - m_0}{m_0} \equiv \frac{\delta m}{m} \simeq \frac{1}{4}\frac{e^2a^2}{(m_0c^2)^2}.$$

Sengupta[2] in 1952 first suggested the possibility that the mass of a free electron might be observed to increase when the electron is allowed to interact with an intense electromagnetic field. This mass-shift effect is just one of many interesting and controversial predictions of theories of intense-field electrodynamics that have appeared over the past few years. Sarachik[3] and Eberly[3] have made comprehensive surveys of these effects, none of which have yet been observed experimentally owing to the difficulty in generating sufficiently intense laser fields.

In 1966 Reiss[4] suggested that an intensity-dependent mass shift could be observed for a bound electron in a plane-wave radio-frequency field. He pointed out that an electron mass increase would affect precision measurements made of spectral lines from a hydrogenlike system. Such spectral lines depend on the electron mass through the Rydberg energy $\mathrm{Ry} = -\frac{1}{2}\alpha^2 mc^2$ and the Bohr magneton $\mu_B = eh/2mc$.

The mass-shift hypothesis for an electron bound in the ground state of a hydrogenlike system is examined here both theoretically and experimentally. It is shown that the hypothesis does lead to shifts of transition frequencies within the ground-state hyperfine structure which do not occur when more conventional treatments of the $\frac{1}{2}e^2a^2$ mass-renormalization term are used. Experimental work of sufficient sensitivity to observe the mass-shift effect has, however, yielded negative results.[5]

II. THEORY OF POSTULATED ELECTROMAGNETIC MASS SHIFT

The following discussion is similar to the one outlined by Reiss[4] for the hydrogen atom, but it is more detailed because it does not neglect effects due to the electron spin. A nonrelativistic wave equation is obtained for hydrogenlike atoms which displays the mass-shift effect explicitly up to and including the Zeeman energy and spin-orbit coupling terms. Perturbation theory is then applied to the ground-state eigenfunction of the approximate Hamiltonian, and the usual Fermi formula for the hyperfine structure (hfs) splitting is obtained, and it also displays the mass shift. Finally, an examination is made of the dependence of the ground-state hfs Zeeman levels on the electron mass.

A. Origin of Mass-Shift Hypothesis

The interaction of a spin-$\frac{1}{2}$ particle with external electric (**E**) and magnetic (**B**) fields can be described by the following equation:

$$(E - e\phi)^2\psi = \{c^2[\mathbf{p} - (e/c)\mathbf{A}]^2 + (mc^2)^2 - ech(\boldsymbol{\sigma}\cdot\mathbf{B} - i\boldsymbol{\alpha}\cdot\mathbf{E})\}\psi, \qquad (2)$$

* Based on a thesis submitted by J. Richard Mowat to the Graduate Division, University of California, Berkeley, 1969, in partial fulfillment of the requirements for the degree of Doctor of Philosophy [LRL Report No. UCRL-19245, 1969 (unpublished)]; work supported by the U. S. Atomic Energy Commission.

† Present Address: Department of Physics, Brandeis University, Waltham, Mass. 02154.

[1] H. R. Reiss and J. H. Eberly, Phys. Rev. **151**, 1058 (1966).

[2] N. D. Sengupta, Calcutta Math. Soc. Bull. **44**, 175 (1952).

[3] E. S. Sarachik, National Aeronautics and Space Administration Report No. NASA-TN-D5205, 1969 (unpublished); J. H. Eberly, in *Progress in Optics*, edited by E. Wolf (North-Holland, Amsterdam, 1969), Vol. 7.

[4] H. R. Reiss, Phys. Rev. Letters **17**, 1162 (1966).

[5] J. R. Mowat, C. E. Johnson, V. J. Ehlers, and H. A. Shugart, Bull. Am. Phys. Soc. **14**, 524 (1969).

where $\mathbf{B}=\nabla\times\mathbf{A}$ and $\mathbf{E}=-(1/c)\partial\mathbf{A}/\partial t-\nabla\phi$ are derived from the magnetic vector potential $\mathbf{A}$ and the electrostatic scalar potential ϕ. $E=ih\partial/\partial t$ and $\mathbf{p}=-ih\nabla$ are the total energy and momentum operators, respectively. The Dirac matrix $\boldsymbol{\alpha}$ is defined by

$$\boldsymbol{\alpha}=\begin{pmatrix}0 & \boldsymbol{\sigma}\\ \boldsymbol{\sigma} & 0\end{pmatrix},$$

where $\boldsymbol{\sigma}$ is a vector comprising the three Pauli matrices, and ψ is a four-component spinor wave function.

Consider the following vector potential:

$$\mathbf{A}=\mathbf{A}_{\rm rot}+\mathbf{A}_s, \tag{3}$$

where

$$\mathbf{A}_{\rm rot}=(a/\sqrt{2})\ \mathrm{Re}[(\hat{y}\pm i\hat{z})e^{-i(\omega t-kx)}]$$

is the vector potential of a circularly polarized plane wave of angular frequency ω and wave number k propagating in the $+x$ direction with velocity $c=\omega/k$ and amplitude a, and

$$\mathbf{A}_s=-B_0y\hat{x}$$

is the vector potential of a uniform, static magnetic field, $\mathbf{B}_s=B_0\hat{z}$. When Eq. (3) is substituted into Eq. (2), one obtains

$$\begin{aligned}(E-e\phi)^2\psi=\{&c^2[\mathbf{p}-(e/c)\mathbf{A}_s]^2\\ &+(mc^2)^2+e^2A_{\rm rot}{}^2-ech(\boldsymbol{\sigma}\cdot\mathbf{B}_s-i\boldsymbol{\alpha}\cdot\mathbf{E}_s)\\ &-2ec\mathbf{A}_{\rm rot}\cdot\mathbf{p}-ech(\boldsymbol{\sigma}\cdot\mathbf{B}_{\rm rot}-i\boldsymbol{\alpha}\cdot\mathbf{E}_{\rm rot})\}\psi,\end{aligned} \tag{4}$$

where the subscripts "rot" and "s" refer to the plane-wave field and the static field, respectively. In order to keep the wave equation time independent, the last three terms in Eq. (4) will be temporarily ignored and considered later in Sec. II D. For the frequencies of interest, the two terms involving $\mathbf{B}_{\rm rot}$ and $\mathbf{E}_{\rm rot}$ are of small magnitude compared to the $e^2A_{\rm rot}{}^2$ term and also compared to the static terms containing $\mathbf{B}_s$ and $\mathbf{E}_s$ (Zeeman effect and spin-orbit coupling). These two time-dependent terms can be satisfactorily accounted for through the use of time-dependent perturbation theory. It will be shown that the $\mathbf{A}_{\rm rot}\cdot\mathbf{p}$ term has a negligible effect on the ground-state hfs transition frequencies.

Once the time dependence in Eq. (4) has been removed, the time variation of ψ can be separated out, and the operator E can be replaced by the total energy, also designated E. For circular polarization,

$$e^2A_{\rm rot}{}^2=e^2\mathbf{A}_{\rm rot}\cdot\mathbf{A}_{\rm rot}=\tfrac{1}{2}e^2a^2.$$

Since $\frac{1}{2}e^2a^2$, like $(mc^2)^2$, is a constant scalar, it was suggested by Reiss[1] that the $\frac{1}{2}e^2a^2$ term serves as a finite mass renormalization, and that one should define an effective mass m_* by

$$(m_*c^2)^2=(mc^2)^2+\tfrac{1}{2}e^2a^2.$$

(Alternative, more conventional, treatments of the $\frac{1}{2}e^2a^2$ term are discussed in Sec. V below.)

As a first step toward obtaining a nonrelativistic wave equation from Eq. (4), we can transfer the $(m_*c^2)^2$ term to the left-hand side, divide by $2m_*c^2$, drop the subscripts s, and introduce the definition

$$W=E-m_*c^2, \tag{5}$$

so the wave equation can be put into the form

$$\begin{aligned}\Big[\frac{1}{2m_*}\Big(\mathbf{p}-\frac{e}{c}\mathbf{A}\Big)^2+e\phi-\frac{eh}{2m_*c}(\boldsymbol{\sigma}\cdot\mathbf{B}-i\boldsymbol{\alpha}\cdot\mathbf{E})\\ -\frac{1}{2m_*c^2}(W-e\phi)^2\Big]\psi=W\psi.\end{aligned} \tag{6}$$

This equation is the same as the one given by Bethe and Salpeter[6] for an electron in an external, static field, except that the electron mass has everywhere been replaced by m_*, the renormalized mass given by Eq. (1).

B. Nonrelativistic Wave Equation

Equation (6) can be transformed, in the spirit of the Foldy-Wouthuysen method, to obtain a nonrelativistic wave equation which contains Zeeman energy and spin-orbit coupling terms which are the same as in the usual nonrelativistic theory except that the electron mass is everywhere replaced by the renormalized mass m_*. The approximation is good only to order $1/m^2$ so the last term in Eq. (6) which is of order $1/m^3$ is neglected. Hence, the starting point for a reduction to a nonrelativistic wave equation is the following:

$$\mathcal{H}_0\psi_0=W\psi_0,$$

where

$$\mathcal{H}_0=\frac{1}{2m_*}\Big(\mathbf{p}-\frac{e}{c}\mathbf{A}\Big)^2+e\phi-\frac{eh}{2m_*c}\boldsymbol{\sigma}\cdot\mathbf{B}+\frac{ieh}{2m_*c}\boldsymbol{\alpha}\cdot\mathbf{E}.$$

The following transformation is introduced:

$$\mathcal{H}_{\rm nr}=e^u\mathcal{H}_0e^{-u},$$
$$\psi_{\rm nr}=e^u\psi_0,$$

where

$$u=-\frac{1}{2m_*c}\boldsymbol{\alpha}\cdot\Big(\mathbf{p}-\frac{e}{c}\mathbf{A}\Big)$$

and $\mathcal{H}_{\rm nr}$ is the nonrelativistic Hamiltonian. The transformation can be accomplished by using the identity

$$\begin{aligned}e^ABe^{-A}=B+[A,B]+(1/2!)[A,[A,B]]\\ +(1/3!)[A,[A,[A,B]]]+\cdots.\end{aligned}$$

After a lengthy but straightforward calculation one obtains

$$\mathcal{H}_{\rm nr}\psi_{\rm nr}=E\psi_{\rm nr},$$

[6] H. A. Bethe and E. E. Salpeter, *Quantum Mechanics of One- and Two-Electron Atoms* (Springer-Verlag, Berlin, 1957), p. 56.

where

$$\mathcal{H}_{nr}=m_*c^2+\frac{1}{2m_*}\left(\mathbf{p}-\frac{e}{c}\mathbf{A}\right)^2+e\phi - \frac{e\hbar}{2m_*c}\boldsymbol{\sigma}\cdot\mathbf{B}-\frac{e\hbar}{2m_*c}\frac{\boldsymbol{\sigma}}{2}\cdot\frac{\mathbf{E}}{m_*c}\times\left(\mathbf{p}-\frac{e}{c}\mathbf{A}\right) + \frac{1}{4}\frac{e\hbar}{2m_*c}\boldsymbol{\sigma}\cdot\frac{\mathbf{p}\times\mathbf{E}}{m_*c}-\frac{e}{8}\left(\frac{\hbar}{m_*c}\right)^2\nabla\cdot\mathbf{E}. \quad (7)$$

This Hamiltonian, except for the replacement of m by m_*, is identical in form to the approximate Hamiltonian obtained when the Foldy-Wouthuysen transformation is applied twice to the linear Dirac equation[7] for an electron in static electric and magnetic fields.

C. Application to Hyperfine Structure

It has just been shown that when time-dependent terms can be neglected, the sole effect of the plane-wave field is to change the electron mass from m to m_* everywhere that it appears in the nonrelativistic Hamiltonian; thus, Eq. (7) displays the mass-shift effect in the Zeeman energy and in the spin-orbit coupling terms. In particular, the Bohr magneton changes by just the amount expected due to an electron mass shift.

The eigenfunctions and eigenvalues of $\mathcal{H}_{nr}$ are the same as in the absence of the plane wave except that the electron rest mass should be replaced everywhere it appears by the renormalized mass m_*. The static perturbation of the $^2S_{1/2}$ hydrogen ground state due to the interaction of the electronic and nuclear spins leads to the usual Fermi formula for the hfs separation ΔW, with the electron mass replaced by m_*. A nucleus possessing a static magnetic dipole moment $\boldsymbol{\mu}_I$ produces a zero-field hfs splitting of the $^2S_{1/2}$ ground state given by

$$\Delta W=\frac{8\pi}{3}\frac{2I+1}{I}\mu_e\mu_I|\psi_0(0)|^2. \quad (8)$$

The interaction of the electronic and nuclear magnetic dipole moments with an external static magnetic field H_0 further splits the $|Fm_F\rangle$ states. The application of degenerate perturbation theory leads to the Breit-Rabi formula[8] for the energy E of the state $|Fm_F\rangle$ as a function of applied field H_0, that is,

$$E=-\frac{\Delta W}{2(2I+1)}-\frac{\mu_I}{I}H_0m_F\pm\frac{\Delta W}{2}\left(1+\frac{4m_F}{2I+1}x+x^2\right)^{1/2},$$

where

$$x\equiv\left(\frac{\mu_I}{I}-\frac{\mu_e}{S}\right)\frac{H_0}{\Delta W}$$

is the magnetic field parameter.

[7] J. D. Bjorken and S. D. Drell, *Relativistic Quantum Mechanics* (McGraw-Hill, New York, 1964), p. 51.

[8] G. Breit and I. I. Rabi, Phys. Rev. **38**, 2082 (1931).

The change in the hfs energy levels due to a change in the electron mass can be obtained by differentiating the Breit-Rabi formula with respect to the electron mass. The hydrogenic wave function can be used to evaluate $|\psi_0(0)|^2$ in the Fermi formula so that the explicit mass dependence of ΔW can be ascertained. Using $|\psi_0(0)|^2=(1/\pi)(Ze^2m_*/\hbar^2)^3$ and $\mu_e=e\hbar/2m_*c$, one finds, with $m_*\simeq m$,

$$\Delta W\propto m^2$$

and

$$\delta(\Delta W)=2(\delta m/m)\Delta W, \quad (9)$$

where $\delta m/m$ is the electron's relative mass shift. In the same fashion, one can write

$$x=\frac{\mu_I}{I}\frac{H_0}{\Delta W}-\frac{\mu_e}{S}\frac{H_0}{\Delta W}\propto c_1m^{-2}+c_2m^{-3},$$

where c_1 and c_2 do not depend upon m. The change in x due to a change in m is

$$\delta x=\frac{\delta m}{m}\frac{H_0}{\Delta W}\left(-\frac{2\mu_I}{I}+\frac{3\mu_e}{S}\right).$$

With these results for $\delta(\Delta W)$ and δx, one obtains, after a straightforward differentiation of the Breit-Rabi formula,

$$\delta E=\frac{\delta m}{m}\left[-\frac{\Delta W}{2I+1}\pm\Delta W\,R \pm\frac{H_0}{2R}\left(-\frac{2\mu_I}{I}+\frac{3\mu_e}{S}\right)\left(\frac{2m_F}{2I+1}+x\right)\right],$$

where

$$R=\left(1+\frac{4m_F}{2I+1}x+x^2\right)^{1/2}.$$

This equation gives the change in energy of the hfs level $|Fm_F\rangle$ due to a relative change $\delta m/m$ in the mass of the electron. This shift is not the same for all hyperfine levels as indicated by the dependence of δE on m_F explicitly and on F through the $\pm$ sign. The frequency shift for a transition between levels of energy E_1 and E_2 due to a shift in the electron mass is given by

$$\delta f=\frac{\delta E_1-\delta E_2}{h}\propto\frac{\delta m}{m}.$$

Hence the shift of a transition frequency is proportional to the relative mass shift. For most cases of experimental interest, a relative mass shift of, say, 10^{-6} results in a relative transition frequency shift of the same magnitude.

D. Consideration of Time-Dependent Terms

In the previous sections, a time-independent Hamiltonian whose eigenfunctions would be stationary states

was obtained by neglecting the following three terms:

$$\mathcal{H}_{\rm rot}=-\frac{e}{m_*c}\mathbf{A}_{\rm rot}\cdot\mathbf{p}-\frac{e\hbar}{2m_*c}(\boldsymbol{\sigma}\cdot\mathbf{B}_{\rm rot}-i\boldsymbol{\alpha}\cdot\mathbf{E}_{\rm rot}).$$

Any time-dependent perturbation such as this can be broken up into its Fourier components, each of which can be studied separately. A typical component may be written in the form

$$\hbar b=Ve^{-i\omega t},\quad V\neq V(t).$$

The resulting transition probabilities and energy-level shifts are proportional to the matrix elements of V between stationary states. The following discussion can therefore be simplified by dropping the factor $e^{-i\omega t}$ from $\mathbf{B}_{\rm rot}$ and $\mathbf{E}_{\rm rot}$.

For a circularly polarized plane wave, $\mathbf{E}=\pm i\mathbf{B}$; therefore the last two terms can be written, dropping the subscript "rot,"

$$\frac{e\hbar}{2m_*c}(\boldsymbol{\sigma}\cdot\mathbf{B}-i\boldsymbol{\alpha}\cdot\mathbf{E})=\frac{e\hbar}{2m_*c}(\boldsymbol{\sigma}\cdot\mathbf{B}\pm\boldsymbol{\alpha}\cdot\mathbf{B})=\boldsymbol{\mu}_e\cdot\mathbf{B}\begin{pmatrix}I & \pm I\\ \pm I & I\end{pmatrix}.$$

When B is 1 G, $\boldsymbol{\mu}_e\mathbf{B}\simeq 6\times10^{-9}$ eV, and this term is much smaller than the hfs separation $\Delta W\simeq 6\times10^{-6}$ eV. The treatment of such a term by time-dependent perturbation theory yields transition probabilities[9] for magnetic dipole transitions when ω is near a transition frequency and small frequency shifts[10] (Bloch-Siegert effect) when it is not. As discussed in Sec. IV below, these frequency shifts are more than two orders of magnitude smaller than possible frequency shifts due to the postulated electron mass shift. It can be shown that this Zeeman energy term will be small compared to the mass-renormalization term whenever $ea\gg\hbar\omega$.

For a circularly polarized plane wave where $\hat{\epsilon}=(1/\sqrt{2})(\hat{y}\pm i\hat{z})$ and $\mathbf{k}=k\hat{x}$, the vector potential can be written

$$\mathbf{A}_{\rm rot}=a\,\mathrm{Re}(\hat{\epsilon}e^{i(\mathbf{k}\cdot\mathbf{r}-\omega t)})=\frac{a}{2\sqrt{2}}[(\hat{y}\pm i\hat{z})(1+ikx)e^{-i\omega t}+(\hat{y}\mp i\hat{z})(1-ikx)e^{+i\omega t}],$$

where the approximation $e^{ikx}\approx 1+ikx$ has been used.

Consider the matrix element

$$\langle n'|\frac{-e}{m_*c}\mathbf{A}\cdot\mathbf{p}|n\rangle\simeq\frac{-ea}{2\sqrt{2}m_*c}[\langle n'|p_y|n\rangle\pm i\langle n'|p_z|n\rangle\mp k\langle n'|xp_z|n\rangle+ik\langle n'|xp_y|n\rangle]\quad(10)$$

of the $e^{-i\omega t}$ term, where $|n\rangle$ stands for $|njIFm_F\rangle$ which is an hfs sublevel of the $|nj\rangle$ eigenstate. Only the ground-state sublevels need be considered. With the aid of the following identities,[11] which hold for S states,

$$\langle m|\mathbf{p}|n\rangle=im_*\omega_{mn}\langle m|\mathbf{r}|n\rangle,\quad(11)$$

$$\begin{aligned}\langle m|r_ip_j|n\rangle&=\tfrac{1}{2}im_*\omega_{mn}\langle m|r_ir_j|n\rangle+\tfrac{1}{2}\langle m|L_k|n\rangle,\\ \langle m|r_ip_i|n\rangle&=\tfrac{1}{2}im_*\omega_{mn}\langle m|r_i^2|n\rangle+\tfrac{1}{2}ih\delta_{mn},\end{aligned}\quad(12)$$

where

$$\omega_{mn}=(E_m-E_n)/\hbar,$$

the first two terms in Eq. (10) become matrix elements of the position operator between two hfs levels. Such matrix elements must vanish because the ground-state hfs levels all have the same parity. An application of Eq. (12) converts the last two terms into the matrix elements of xy and xz. This is essentially an electric quadrupole matrix element which vanishes in the case of a $^2S_{1/2}$ ground state because there can be no electric quadrupole interaction within a $J=\frac{1}{2}$ state.

The mass-shift effect under investigation has been interpreted as a transition-frequency shift. Transition-frequency measurements are, in essence, the determination of the frequency at which the transition probability is a maximum. It is therefore appropriate to consider the effect on the transition probability of a nonresonant perturbation $Ve^{-i\omega t}$. Ramsey[12] has analyzed the situation that occurs when two or more rotating perturbations, only one of which is resonant, are applied simultaneously to a system of energy levels whose separation frequencies are fixed. The simultaneous presence of the nonresonant perturbation given above, together with a resonant perturbation, shifts the peak transition probability so that it occurs at a frequency ω_0' given by

$$\omega_0'=\omega_0+\sum_i\frac{|\langle i|V|1\rangle|^2}{\hbar^2[(E_i-E_1)/\hbar-\omega]}+\sum_j\frac{|\langle 2|V|j\rangle|^2}{\hbar^2[(E_2-E_j)/\hbar-\omega]},\quad(13)$$

where

$$\omega_0=(E_2-E_1)/\hbar$$

is the frequency corresponding to the peak in the transition probability in the absence of the nonresonant perturbation. The sum over i (j) includes those states which can be connected by the perturbation to the initial (final) state.

If only the ground-state hfs sublevels are included in the summations, then, as shown above, all the matrix elements vanish, and there is no frequency shift.

When states of other energy levels are included in the summations, two simplifications arise. The nonresonant microwave frequency chosen for the experiment is 3 GHz, which is negligible compared to the ^{133}Cs energy separation $6^2S_{1/2}-6^2P_{1/2}$ which is about 3.3×10^5 GHz. Hence it is possible to replace ω's appearing in the denominators by zero. Secondly, the two hfs states $|1\rangle$

[9] I. I. Rabi, Phys. Rev. **51**, 652 (1937).
[10] F. Bloch and A. Siegert, Phys. Rev. **57**, 522 (1940).
[11] See Ref. 6, pp. 252 and 279.
[12] N. F. Ramsey, Phys. Rev. **100**, 1191 (1955); M. Mizushima, *ibid.* **133**, A414 (1964).

and $|2\rangle$ each have the same radial wavefunction as do all the states of a given fine-structure level $|nlj\rangle$. It is therefore possible to write the frequency shift as

$$\omega_0'-\omega_0=\sum_{n,l,j}\left(\frac{|\langle nlj|V|0\rangle|^2}{\hbar(E_{nlj}-E_0)}-\frac{|\langle 0|V|nlj\rangle|^2}{\hbar(E_{nlj}-E_0)}\right)=0,$$

where $|0\rangle$ represents the ground state. Hence, to the extent that the frequency of the nonresonant perturbation is small compared to the energy separation, the $\mathbf{A}_{\rm rot}\cdot\mathbf{p}$ term has a negligible effect on transition frequencies within the ground state hfs.

III. DESCRIPTION OF EXPERIMENT

A. Experimental System

The atomic-beam magnetic-resonance technique was used in this search for an electron mass-shift effect in ^{133}Cs. Although the theory of the electron mass shift was developed in Sec. II with the hydrogen atom in mind, it should apply to alkali atoms whenever the valence electron experiences an electrostatic potential which is a function of radial position only (central field approximation). The noncentral magnetic dipole interaction has already been accounted for by perturbation theory and has led to the hyperfine interaction described by the Fermi formula. The spherical symmetry of the $^2S_{1/2}$ electronic state forbids the existence of any multipole interactions beyond electric monopole and magnetic dipole.

Breit[13] and Kopfermann[14] have summarized some of the correction factors which should be applied to the Fermi formula before it is used to deduce alkali nuclear magnetic dipole moments from measured hyperfine energy separations. When these correction factors are taken into consideration, one obtains

$$\delta(\Delta W)=1.96(\delta m/m)\Delta W,$$

which differs by only 2% from the result obtained in Eq. (9) assuming hydrogenic wave functions and no corrections to the Fermi formula.

The nuclear spin angular momentum I of ^{133}Cs is $\frac{7}{2}\hbar$ and the total electronic angular momentum in the ground state is $J=S=\frac{1}{2}\hbar$. The total angular momentum $\mathbf{F}=\mathbf{I}+\mathbf{J}$ can assume in this case only the values $F=I+J=4$ and $F=I-J=3$. The projection of the total angular momentum onto a preferred direction in space is given by the magnetic quantum number $m_F=F$, $F-1$, ..., $-(F-1)$, $-F$. Figure 1, which is a plot of the Breit-Rabi formula in frequency units, shows how these levels are split by a static, externally applied magnetic field H_0. Effects of field inhomogeneities can be minimized by working at fields where the transition frequencies are only weakly dependent upon H_0. At those magnetic fields where $df/dH_0=0$ (field-independent points), the transition frequency f is independent, to first order, of magnetic field H_0. Table I is a list of the field-independent $\Delta F=\pm1$ transitions for ^{133}Cs. Four are of the σ type ($\Delta m_F=0$), while six are of the π type ($\Delta m_F=\pm1$). The six π transitions occur in three doublets which are labeled a, b, and c in Fig. 1. These three doublets were chosen for extensive study in the search for an electron mass shift.

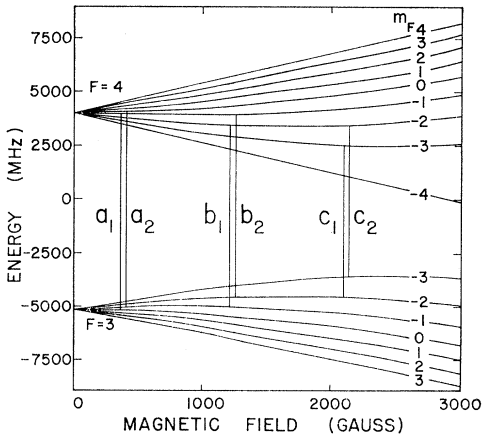

FIG. 1. Breit-Rabi diagram for ^{133}Cs. The three $\Delta F=1$, $\Delta m_F=\pm1$ field-independent doublet transitions are shown; the labels correspond to the notation in Table I.

B. Apparatus

A standard flop-in atomic-beam magnetic-resonance apparatus[15] utilizing the separated-oscillatory-field technique[16] is used to investigate shifts of hfs transition frequencies that occur as a cesium beam traverses a microwave cavity. Cesium atoms are produced in a resistance-heated steel oven by the reaction of calcium

TABLE I. ^{133}Cs field-independent $\Delta F=1$ transitions. The designations a, b, or c refer to the transitions labeled in Fig. 1; these are the transitions for which frequency shifts were observed.

Designation	Transition (F,m_F)	Type	Field-independent parameters: Field (G)	Field-independent parameters: Frequency (MHz)
	(4,0) ↔ (3,0)	σ	0	9192.631770
a_1	(4, −1) ↔ (3,0)	π	416	9119.6
a_2	(4,0) ↔ (3, −1)	π	417	9119.1
	(4, −1) ↔ (3, −1)	σ	820	8900.7
b_1	(4, −2) ↔ (3, −1)	π	1252	8509.5
b_2	(4, −1) ↔ (3, −2)	π	1253	8508.1
	(4, −2) ↔ (3, −2)	σ	1640	7961.0
c_1	(4, −3) ↔ (3, −2)	π	2104	7115.3
c_2	(4, −2) ↔ (3, −3)	π	2105	7112.9
	(4, −3) ↔ (3, −3)	σ	2460	6080.4

[13] G. Breit, Phys. Rev. 42, 348 (1932).
[14] H. Kopfermann, *Nuclear Moments* (Academic, New York, 1958), p. 136.
[15] J. R. Zacharias, Phys. Rev. 61, 270 (1942); P. A. Vanden Bout, V. J. Ehlers, W. A. Nierenberg, and H. A. Shugart, *ibid.* 158, 1078 (1967).
[16] N. F. Ramsey, Phys. Rev. 78, 695 (1950).

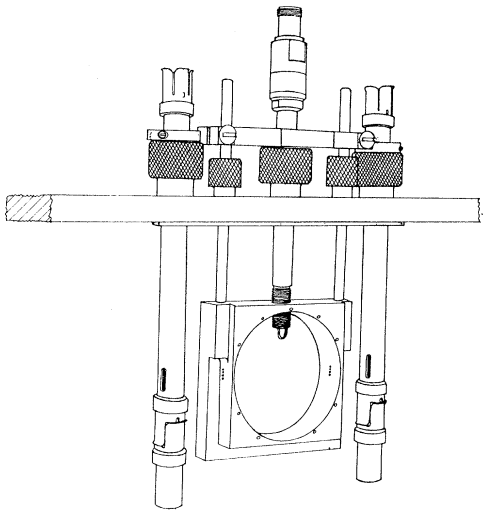

FIG. 2. Sketch of the microwave cavity and the two separated transition hairpins.

metal with a cesium halide, e.g.,

$$Ca+2CsCl+heat \rightarrow CaCl_2+2Cs.$$

1. Cavity-Hairpin Assembly

The actual experiment is performed in the constant-field region where appropriate resonant and non-resonant oscillating fields are introduced through the cavity-hairpin assembly. Figure 2 is a sketch of the assembly with the cover removed to show the inside of the cavity. The beam passes from left to right, and the static field H_0 is at right angles to the cavity faces. The entrance and exit apertures in the cavity each consist of four 0.055-in.-diam holes which serve to collimate the beam.

The cavity is resonant at 2.921 GHz (TM_{010} mode), and has an unloaded Q of 4200 ± 200 (determined by a least-squares analysis of the power absorption curve). The rf magnetic field lines inside the cavity are concentric with the cylinder axis. H_{rf} is zero at the center and rises to a maximum value about three-quarters of the way out to the wall. At the wall, H_{rf} has a nonzero value. The beam experiences an oscillating rf magnetic field that is perpendicular to the static field H_0. The electric field and vector potential are directed parallel to the cavity axis and perpendicular to the faces. The beam hence experiences an oscillating rf electric field and vector potential that are parallel to the static magnetic field H_0.

A high-powered continuous-wave microwave signal produced by a mechanically tuned magnetron is fed into the constant-field region via a $\frac{1}{2}$-in. 50-Ω rigid coaxial transmission line and is inductively coupled to the cylindrical cavity. The coupler designed for this purpose is exposed in Fig. 2.

The hairpins consist of terminated $\frac{5}{8}$-in. 50-Ω rigid coaxial transmission lines. They produce an oscillating magnetic field at the beam which is, for the most part, at right angles to H_0, and is appropriate for stimulating π transitions. Fields oscillating in phase and at a frequency equal to the transition frequency of interest are established in the two hairpins which are separated by a distance of 6 in. (center to center).

2. Radio-Frequency Equipment

a. Transition Frequencies. Microwave signals at cesium transition frequencies are generated by a phase-locked, continuously operating klystron and fed to the separated hairpins as illustrated in Fig. 3. A very stable reference oscillator provides the fundamental comparison frequency. This comparison is made by a syncriminator which applies a correction voltage to the reflector of the klystron. A traveling-wave tube amplifies the klystron signal which is then divided, one-half being sent directly to one hairpin, and the other half being sent through a phase shifter and variable attenuator to the other hairpin. The attenuator allows one to equalize the rf field amplitudes in the two hairpins. The phase shifter provides a way of equalizing the phase of the signals reaching the hairpins by changing the electrical length of the transmission line leading to one of them. The two signals are judged to be in phase when a symmetrical Ramsey pattern is obtained; see Fig. 4.

Klystron frequencies are measured directly with a digital frequency counter which is capable of counting frequencies up to 12.4 GHz. Both the reference oscillator and the counter are referred to the same 100-kHz quartz crystal oscillator which is, in turn, continuously compared with the 60-kHz standard frequency broadcast by the National Bureau of Standards's station WWVB, Fort Collins, Colo. Because of the high stability of the 100-kHz reference, the precision of frequency measurements was determined by the uncertainty of ±1 in the last place of the counter display.

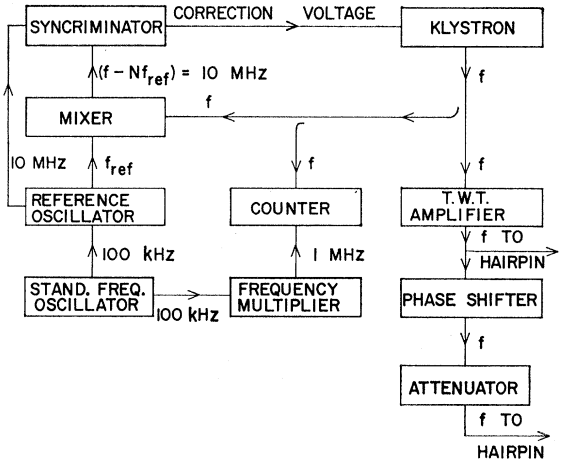

FIG. 3. Radiofrequency arrangement for driving the separated transition hairpins.

b. Magnetron-Cavity Circuit. The circuit used to power the cavity is shown schematically in Fig. 5. The signal from an isolated, continuously operating 100-W magnetron can be fed either to the cavity or to a dummy load capable of absorbing 175 W. Both input and return power are sampled with a 20-dB dual directional coupler and measured with the same power meter. The magnetron frequency is measured directly with a digital frequency counter.

Insertion losses of all circuit components (including cables) were measured, so that the actual power absorbed by the cavity could be determined from power meter readings of input and return power. These measurements agreed with manufacturers's specifications when given.

3. *Effective Fields of TM_{010} Cavity*

The effective fields experienced by an atomic beam that traverses an evacuated TM_{010} cylindrical cavity along a diameter midway between the ends are[17]

$$E=|E|e^{-i\omega t},\quad B=i|B|e^{-i\omega t},\quad A=-i|A|e^{-i\omega t},$$

where

$$|E|^2=(0.455\pm0.023)E_0^2,$$
$$|B|^2=(0.212\pm0.009)E_0^2,$$
$$|A|^2=(0.455\pm0.023)\times(c/\omega)^2E_0^2,$$

and

$$E_0^2=203PQ\nu_0/lc^2.$$

P is the power absorbed in the cavity walls in erg/sec, Q is the unloaded Q, ν_0 is the resonant frequency in Hz, l is the length in cm, and c is the speed of light in vacuum. The numerical factors in the above equations were calculated by averaging the squares of the fields along a cavity diameter. The errors quoted are intended to account for the variation of the fields over the height of the beam (about $\frac{1}{4}$ in.). When P is expressed in W, ν_0 in GHz, and l in cm, the amplitude of the vector potential becomes

$$|A|^2=0.023PQ/\nu_0 l$$

and the electron relative mass shift is, for $P=1$ W, $Q=4200$, $\nu_0=2.921$ GHz, and $l=1.91$ cm,

$$\frac{\delta m}{m}=\frac{1}{2}\frac{e^2|A|^2}{(mc^2)^2}=4.03\times10^{-9}\frac{PQ}{\nu_0 l}\simeq3\times10^{-6}.$$

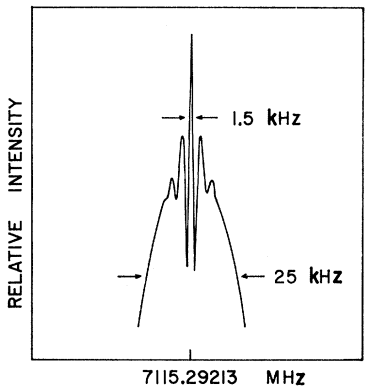

FIG. 4. Representative Ramsey pattern used in measurements of frequency shifts.

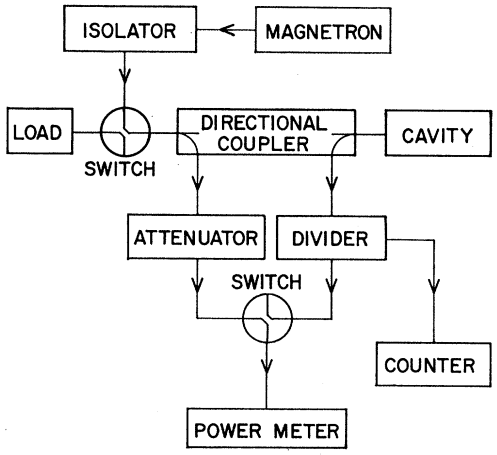

FIG. 5. Circuit used to power the microwave cavity.

C. Experimental Procedure

At the start of each run, the magnetron was set for maximum output and tuned to the cavity resonant frequency. After several minutes the water-cooled cavity came to equilibrium, and the return power was steady and less than 1% of the input power. The signal observed at the detector for a constant static magnetic field, constant power input to the cavity, but varying hairpin frequency, is shown in Fig. 4.

A measurement was then made of the position of the center of the central peak in the Ramsey pattern. This was done by averaging frequency readings taken at two or three positions symmetrically located on each side of the central peak. Hence, four or six frequency measurements, when averaged, gave one value for the center frequency. This procedure was performed ten times and the average of the ten center frequencies so measured was taken to be the best value for the transition frequency. Without changing the cavity input power, the transition frequency of the other member of the doublet was then determined in the same manner. The cavity power was then decreased, and, after equilibrium was achieved, the two frequencies were again measured. In this way the transition frequency was measured for five values of cavity power, including zero power. The five measurements of each transition frequency were then fit by a least-squares procedure to a straight line with each point weighted in inverse proportion to its standard deviation; see Fig. 6.

[17] J. D. Jackson, *Classical Electrodynamics* (Wiley, New York, 1962), p. 254; J. R. Mowat, Ph.D. thesis, LRL Report No. UCRL-19245, 1969 (unpublished).

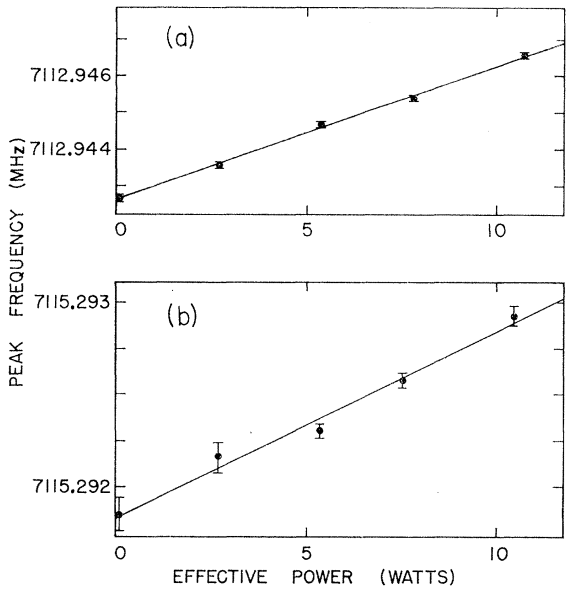

FIG. 6. Transition frequency versus effective rf cavity power for the 2100-G doublet, using a cavity frequency of 2921 MHz. Curve (a) is the $(4, -2) \leftrightarrow (3, -3)$ transition and curve (b) is the $(4, -3) \leftrightarrow (3, -2)$ transition.

IV. EXPERIMENTAL RESULTS

The results of 27 measurements of ^{133}Cs hfs transition frequency shifts induced by the fields of a high-Q microwave cavity reveal no evidence for an electron mass shift. The measurements were sensitive enough to detect the Bloch-Siegert effect, which is more than two orders of magnitude smaller than the expected mass-shift effect.

Figure 6 is a representative plot of transition frequency versus cavity power for one of the three field-independent doublets studied and indicates how well the data fit a straight-line dependence. The effective cavity power is obtained by considering (a) the calibration of the absorbed cavity power versus the power meter reading, (b) the factor arising from the cavity filling only part of the measuring region, and (c) the characteristics of the method of sensing a change in energy in the region between the separated transition loops.

Table II summarizes all experimental results. Each measurement listed is the average for four or five runs; the errors given represent the repeatability of the shifts and the uncertainties associated with Q, with the power P, and with the averages of the cavity fields over the beam height. The designations a_1, a_2, etc., refer to the notation of Table I and Fig. 1. The observed shifts $S_{\rm obs}$ are given in both Hz/W and Hz/G^2 for comparison with the expected mass-shift effect $S_{\rm ms}$ and Bloch-Siegert effect $S_{\rm BS}$. In addition to the discrepancy in absolute size (more than two orders of magnitude) between the observed shifts and those expected due to an electron mass shift, there is also a striking discrepancy in the relative size of the shifts of the two 2100-G transitions c_1 and c_2. If these shifts were due to an increase in the electron mass, the two should be equal (to within a few percent), whereas they differ by a factor of about 3.7.

On the other hand, there is good agreement between the six observed shifts and those expected on the basis of a many-level Bloch-Siegert effect. This effect amounts to a shift in the maximum transition probability (i.e., the central peak of the Ramsey pattern) due to the presence of a nonresonant perturbation. Evidently, the rf magnetic field in the cavity has been slightly overestimated, causing the calculated Bloch-Siegert shifts to be somewhat larger than the listed measurements. The relative sizes of the six measurements agree completely, within experimental error, with the calculated Bloch-Siegert shifts.

An oscillating magnetic field $H_{\rm rf}$, oriented at right angles to a uniform C-field H_0, shifts a given magnetic-dipole transition frequency f by[12]

$$\Delta f=\left(g_J\frac{\mu_0}{h}\frac{H_{\rm rf}}{2}\right)^2\sum_j\sum_i\left\{\frac{|\langle i|J_x|1\rangle|^2}{[(E_i-E_1)/h-\nu_j]}+\frac{|\langle 2|J_x|i\rangle|^2}{[(E_2-E_i)/h-\nu_j]}\right\}, \quad (14)$$

where $(E_2-E_1)/h$ is the transition frequency under study. The index j takes on two values corresponding to $\nu_j=\pm\nu_0$, the frequency of the nonresonant perturbation. The index i runs through all the states that can be reached by a π-type transition from either the initial or the final state. This many-level Bloch-Siegert effect is seen to be proportional to the square of the rf magnetic field and hence is a linear function of power.

Perhaps the quickest way to test whether one is observing the Bloch-Siegert effect or the mass-shift effect is to choose a cavity mode for which the mass-shift theory predicts large, positive, and equal frequency shifts for the two members of a π doublet, while the expected Bloch-Siegert shifts are small, negative, and unequal. Such is the case for the 2100 G doublet when the cavity frequency is 7930 MHz, and $H_{\rm rf}$ is perpendicular to H_0. Seven runs were made at this frequency using a TM_{210} cavity powered by a mechanically tuned magnetron. Figure 7 is a plot of transition frequency versus power for one such run. The frequency shifts

TABLE II. Comparison of observed shifts ($S_{\rm obs}$) with predicted shifts for the mass-shift effect ($S_{\rm ms}$) and the Bloch-Siegert effect ($S_{\rm BS}$).

Transition	Frequency (MHz)	$S_{\rm ms}$ (10^3 Hz/W)	$S_{\rm obs}$ (Hz/W)	$S_{\rm obs}$ (Hz/G^2)	$S_{\rm BS}$ (Hz/G^2)
a_1	9119.6	55±4	154±9	50±3	60
a_2	9119.1	55±4	154±15	50±3	62
b_1	8509.5	52±4	172±9	56±3	61
b_2	8508.1	52±4	191±7	62±4	72
c_1	7115.3	43±3	94±6	30±2	38
c_2	7112.9	43±3	349±46	113±8	150

are clearly negative and unequal. The results of these runs reinforce the conclusion drawn from Table II, namely, that all shifts observed can be interpreted as Bloch-Siegert shifts.

V. CONCLUSION: WHY MASS-SHIFT EFFECT WAS NOT OBSERVED

The discussion of Sec. II was concerned with a hydrogenlike atom in a *circularly* polarized plane-wave field, while the oscillating fields experienced by a beam atom traversing a diameter of a TM_{010} cavity are roughly similar to those of a *linearly* polarized plane wave. Such a wave can be represented by

$$\mathbf{A}=\hat{\epsilon}ae^{i(kx-\omega t)},$$
$$A^2=\tfrac{1}{2}a^2[1+\cos 2(kx-\omega t)],$$

where $\hat{\epsilon}$ is the (real) polarization vector. For a linearly polarized plane wave, the terms involving the vector potential in Eq. (4) become

$$e^2A_{\rm rot}{}^2-2ec\mathbf{A}_{\rm rot}\cdot\mathbf{p}$$
$$=\tfrac{1}{2}e^2a^2+\tfrac{1}{2}e^2a^2\cos 2(kx-\omega t)-2eca\hat{\epsilon}\cdot\mathbf{p}e^{i(kx-\omega t)}.$$

The constant term corresponds to the $\frac{1}{2}e^2a^2$ mass-renormalization term for circular polarization. The second and third terms will be analyzed using time-dependent perturbation theory. The $\cos 2(kx-\omega t)$ term can be treated as two oppositely rotating perturbations of frequencies $\pm 2\omega$. Thus, dividing by $2mc^2$,

$$[(e^2a^2)/(4mc^2)]\cos 2(kx-\omega t)=V_1e^{-i\omega_1 t}+V_2e^{-i\omega_2 t},$$

where $\omega_1=2\omega$ and $\omega_2=-2\omega$ and

$$V_1\cong[(e^2a^2)/(8mc^2)](1+i2kx-4k^2x^2),$$
$$V_2\cong[(e^2a^2)/(8mc^2)](1-i2kx-4k^2x^2).$$

The same arguments used in Sec. II D to eliminate the $\mathbf{A}_{\rm rot}\cdot\mathbf{p}$ term for the case of circular polarization can be invoked to show that the first two terms in the expansions of V_1 and V_2 and the $\hat{\epsilon}\cdot\mathbf{p}$ term cause no shift of hfs transition frequencies. The following crude calculation shows that the first nonvanishing frequency shifts arising from V_1 and V_2 are negligibly small. For a two-level system,[12]

$$\omega_0'-\omega_0=\frac{2|\langle 1|V|2\rangle|^2}{\hbar^2(\omega_0-\omega)}.$$

Since the hfs states $|1\rangle$ and $|2\rangle$ have the same radial wave functions,

$$|\langle 1|V|2\rangle|^2=(e^2a^2k^2/2mc^2)^2|\langle x^2\rangle|^2.$$

With $|H_{\rm rf}|=|ka|$ and $\langle x^2\rangle\approx a_0{}^2=[\hbar^2/(me^2)]^2$, the shift becomes

$$\omega_0'-\omega_0\approx\frac{2(\mu_0H_{\rm rf}/h)^2}{\omega_0-\omega}\left(\frac{\mu_0H_{\rm rf}}{\alpha mc^2}\right)^2;$$

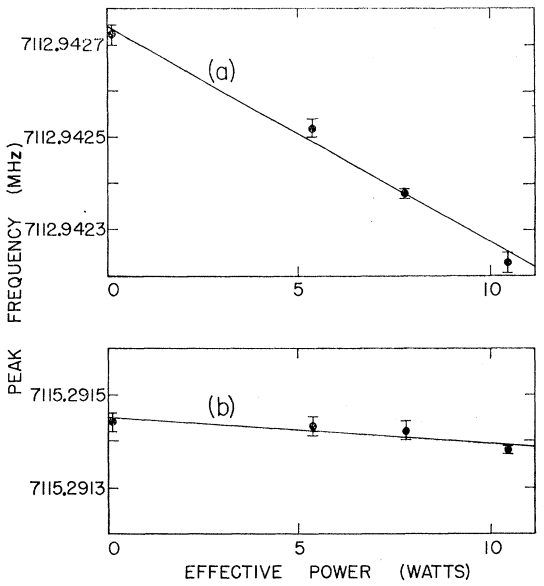

FIG. 7. Transition frequency versus effective rf cavity power for the 2100-G doublet, using a cavity frequency of 7930 MHz. Curve (a) is the $(4,-2)\leftrightarrow(3,-3)$ transition and curve (b) is the $(4,-3)\leftrightarrow(3,-2)$ transition.

but $[2(\mu_0H_{\rm rf}/h)^2]/(\omega_0-\omega)$ is the Bloch-Siegert shift. Hence, the largest shift caused by the cosine term is smaller than the Bloch-Siegert effect by the factor $(\mu_0H_{\rm rf}/\alpha mc^2)^2$, and is therefore negligible. The results of Sec. II hence apply to the case of linear polarization as well as to the case of circular polarization.

There are three ways in which the constant term $e^2A_{\rm rot}{}^2$ appearing in Eq. (4) may be handled: (i) Combine $e^2A_{\rm rot}{}^2$ with $(mc^2)^2$ to get a renormalized mass, as was done in Sec. II; (ii) combine $e^2A_{\rm rot}{}^2$ with $W=E-mc^2$ and get the same shift for all energy levels; or (iii) leave the term in the equation until after the nonrelativistic approximation has been obtained, treat it by perturbation theory, and get an equal shift of all energy levels. The more conventional alternatives, (ii) and (iii), are equivalent to order $1/m^2$, i.e., when the relativistic term $(1/2mc^2)(W-e\phi)^2$ is neglected. Constant perturbations that shift all energy levels by the same amount cannot cause frequency shifts. In the light of our negative experimental results it appears that the $\frac{1}{2}e^2a^2$ term should be considered as a constant perturbation, rather than as a mass shift.

ACKNOWLEDGMENTS

We acknowledge Professor Charles Schwartz, Professor P. G. H. Sandars, and Professor W. A. Nierenberg for useful discussions, and E. S. Sarachik for a careful reading of the manuscript and helpful suggestions.